A Test of the Simulation of Tropical Convective Cloudiness by a Cloud-Resolving Model

Mario A. Lopez, Dennis L. Hartmann, Peter N. Blossey, Robert Wood, Christopher S. Bretherton, and Terence L. Kubar

Department of Atmospheric Sciences
University of Washington
Seattle, Washington 98195

September 21, 2007
Submitted to J. Climate

Corresponding author address: Dennis L. Hartmann, Department of Atmospheric Sciences, University of Washington, Seattle, WA 98195-1640
E-mail: dhartm@washington.edu

Abstract

The distributions of tropical high clouds produced by a doubly periodic three-dimensional cloud-resolving model are compared with satellite observations. The model is forced with steady forcing characteristic of tropical Pacific convective regions, and the model clouds are compared with satellite observations for the same regions. Clouds are divided into categories that represent convective cores, moderately thick anvil clouds and thin high clouds. The statistics of these clouds and their relationship to the precipitation rate are computed in a similar way for the model data and for observations from the Earth-orbiting satellites. The model produces a good simulation of the relationship between the precipitation rate and optically thick cold clouds that represent convective cores. The model also does a reasonable job of simulating the abundance of thin cold clouds in the East and West Pacific ITCZ regions. The model produces too little anvil cloud by a factor of about 4, however. The observations show probability density functions for OLR and albedo with maxima that correspond to extended upper level cold clouds, whereas the model does not. The sensitivity to model parameters of the simulation of anvil cloud area per unit of precipitation is explored using a two-dimensional model. A set of cloud physics parameters is found that produces anvil cloud with realistic amounts and sensitivity to the precipitation rate, while preserving the good simulation of thick and thin cloud.

1. Introduction

The role of clouds remains one of the primary uncertainties in projections of future climates (Bony *et al.*, 2006: IPCC, 2007). Clouds and water vapor have a strong influence on the radiation budget of Earth, and it is still unclear how cloud properties respond to global climate change. The Tropics account for half of the surface area of Earth and much more than half of the Earth's greenhouse effect. Tropical deep convection is important in setting the relationship between surface temperature and the radiation balance at the top of the atmosphere (Hartmann *et al.*, 1992). High, cold clouds are particularly interesting because the extended upper level clouds associated with tropical convection greatly influence both longwave emission and absorbed solar radiation, although their effect on the net energy balance is often much less than their individual effects on longwave and solar radiation (Hartmann *et al.*, 2001).

Deep convective cells occupy a very small fraction of the tropical area. The extended upper level clouds that vary from thick stratiform anvil clouds to thin cirrus clouds have more cloud mass and area and are much more important in the radiative balance of Earth. Anvil clouds associated with intense tropical convective systems are known to have long lifetimes and to cover large areas, accounting for a significant fraction of the precipitation produced by such systems (Leary and Houze, 1980). Large mesoscale convective systems over the Western Pacific Warm Pool form long lived structures called "super clusters" which can extend for thousands of kilometers and last as long as 2 days (Mapes and Houze, 1993: Chen *et al.*, 1996), and the anvil clouds associated with such systems have a large effect on tropical climate.

The upper level anvil clouds are important not only radiatively, but also in setting the structure of the vertical heating profile in the tropics. Rainfall from the anvils

evaporates as it falls through clear air below and this process makes the vertical profiles of heating and vertical velocity much more top heavy (Houze, 1982). It is reasonable to suppose that the heating profile of organized convection in the tropics shapes the large-scale vertical velocity in the Tropics (Mapes *et al.*, 2006), and if so, this has significant implications for the large scale flow (Hartmann *et al.*, 1982: Lin *et al.*, 2004b: Schumacher *et al.*, 2004). The vertical velocity profile is also very important in determining the gross moist stability and other diagnostics of the interaction of convection with large-scale thermodynamics (Back and Bretherton, 2006). The interaction between organized deep convection and large-scale vertical motion is a central issue in tropical meteorology.

Several hypotheses have been put forward regarding the possible role of tropical convective clouds in climate sensitivity. The Thermostat Hypothesis (Ramanathan and Collins, 1991) suggests that the strong reflection of solar radiation by anvil clouds over the warmest SSTs provide an upper limit on the SST, but the steps that lead from surface shading by tropical convective clouds to a limit on SST have been questioned by many other authors (Fu *et al.*, 1992: Hartmann and Michelsen, 1993: Lau *et al.*, 1994: Del Genio *et al.*, 2005) . In the Iris Hypothesis, Lindzen et al. (2001) suggest that anvil clouds have a warming effect and that their spatial coverage relative to convective cores will decrease as SSTs warm, possibly providing a negative climate feedback, but many studies have found contrary evidence (Chambers *et al.*, 2002: Del Genio and Kovari, 2002: Fu *et al.*, 2002: Hartmann and Michelsen, 2002: Lin *et al.*, 2002: Lin *et al.*, 2004a: Rapp *et al.*, 2005: Lin *et al.*, 2006). Hartmann and Larson (2002) have proposed the Fixed Anvil Temperature (FAT) Hypothesis, which suggests that anvil cloud temperature

will remain constant as climate changes, providing an important large-scale constraint on clouds during climate change. The FAT hypothesis has been supported by cloud-resolving modeling (Kuang and Hartmann, 2007) and observations (Kubar *et al.*, 2007: Xu *et al.*, 2007). Hartmann et al (2001) have proposed that the net radiative effect of tropical convective clouds on Earth's energy balance can never be very different from that of surrounding non-convective regions under conditions that prevail in the warm pool region of the West Pacific. They also point out that the distribution of optical depth in cold cloud populations is very important in determining their net cloud radiative forcing, which is part of the motivation for focusing here on the distribution of optical depth of cold clouds.

Each of the hypothesized effects described above is plausible, but it is unclear how they interact and whether other effects that we have not yet considered might supercede them (Stephens, 2005). Observational studies and modeling studies can shed light on these issues, but an important focus should be to bring models and data together in a way that tests our understanding and the ability of models to simulate the relevant physical processes.

Although some climate models have an upper level ice cloud parameterization tied to the convection scheme and can produce reasonable simulations of upper level clouds (Comstock and Jakob, 2004), upper level ice clouds are often deficient in amount or spatial structure (Li *et al.*, 2005), and others show clear deficiencies related to the proper simulation of tropical anvil clouds (Ringer and Allan, 2004). No global climate models currently have a tested parameterization for anvil cloud dynamics, although GCM parameterizations are beginning to consider more explicit incorporation of the effects of

mesoscale circulations and anvil cloud formation (Donner *et al.*, 2001). It has been proposed that a way forward is to use much greater spatial resolution, perhaps with cloud-resolving models (CRM) embedded within a more coarsely gridded global climate model (Grabowski, 2001: Randall *et al.*, 2003a). In this manner the interactions between mesoscale circulations, cloud physics and radiation may be incorporated explicitly in a global climate model for a computational cost that is less than a global cloud-resolving model. This is especially important in the Tropics, where large-scale forcing of convection is less dominant than in midlatitudes, and self-organization of convection is critical (Su *et al.*, 2000: Grabowski, 2003b). An important step is to verify that CRM's of the type proposed for inclusion in climate models can simulate key processes realistically and produce realistic cloud properties.

Cloud Resolving Models are designed to simulate convection explicitly. They have much finer horizontal resolution than GCMs, typically 1 to 5 km compared with hundreds of km in GCMs. At higher spatial resolution, the vertical motions of cloud-scale convective plumes are assumed to be resolved using the prognostic equations of motion, so a convective parameterization is not used. Cloud microphysical processes and sub-grid turbulent transport must still be parameterized, however. CRMs can be used to compute radiative-convective equilibrium (Tompkins and Craig (1998)), or they can be driven with specified large-scale forcing.

CRM validation methodologies have involved comparing the results of both CRMs and Single Column Models (SCMs) to observations. Luo et al. (2005) demonstrate that the UCLA/CSU CRM produces more realistic cirrus cloud properties than the SCM version of the Global Forecast System Model. Using a variety of both CRMs and SCMs

to simulate ARM observations, Randall et al. (2003b) demonstrate that CRMs produce smaller biases in vertical profiles of water vapor, temperature, and cloud occurrence than SCMs. Because CRMs perform better than SCMs in radiative convective equilibrium simulations, it has been proposed that GCM simulations may improve if their convective parameterization schemes are replaced with a CRM embedded in each grid cell. These schemes have shown promise in helping models produce realistic Madden-Julian Oscillations (Grabowski, 2003c: Randall *et al.*, 2003b). Ovtchinnikov et al. (2006) show that a GCM using an embedded CRM convective scheme produces too little high cloud compared to observations, however. Wyant et al. (2006b) compare clouds produced by a GCM using super parameterization to ISCCP data, showing that in different dynamical regimes the model tends to either over-predict or under-predict cloud fraction. Both GCMs with embedded CRMs and global cloud-resolving GCMs are beginning to be used to evaluate climate sensitivity (Miura *et al.*, 2005: Wyant *et al.*, 2006a).

More effort should be devoted to methodologies that compare CRMs with observational data directly, especially their ability to simulate realistic clouds and their relation to the top-of-atmosphere (TOA) radiation balance. Comparing the Advanced Regional Prediction System/Langley Research Center CRM to satellite observations, Eitzen and Xu (2005) showed differences in probability density functions (PDFs) of albedo and outgoing longwave radiation (OLR) between large cloud objects in the model and in observations. Luo et al. (2007) found that a CRM intended for use as part of a super parameterization tended to underestimate higher albedos. In another CRM verification study, Blossey et al. (2007) compared the System for Atmospheric Modeling

(SAM) to KWAJEX observations, showing persistent biases in albedo and OLR due to an insufficient amount of high clouds during periods of low to moderate precipitation.

Here we provide an example of bringing satellite data to bear on testing the simulation of tropical convective cloud structure by a cloud-resolving model. This comparison focuses on the necessity of properly simulating the distribution of optical depth in cold clouds. We compare the distributions of high clouds produced by the SAM model run in a tropical domain with distributions observed from space by the Moderate Resolution Imaging Spectrometer (MODIS) instrument, using the Advanced Microwave Scanning Radiometer (AMSR) instrument to sort the data by rain rate. Particular attention will be given to simulating the correct distribution of optical depth for cold clouds. PDFs and domain averages of albedo and OLR are also examined to help quantify the relationship between clouds and the TOA energy budget in the model. Section 2 describes the observational methodology. Sections 3 and 4 present three-dimensional (3-D) simulations and results. Section 5 introduces two-dimensional (2-D) methodology that is used to test how changes to the model may affect anvil cloud amount, and Section 6 details these 2-D experiments. Finally, Section 7 offers discussion and conclusions.

2. Observational Methodology

The goal is to compare cloud-resolving model simulations of tropical convection with satellite observations to test the validity of the model. The observational methodology follows that of Kubar et al. (2007) (hereafter KHW), in which coincident measurements of precipitation from the Advance Microwave Scanning Radiometer

(AMSR) (Wilheit *et al.*, 2003) and cloud optical depth and cloud top temperature measurements from the Moderate Resolution Imaging Spectrometer (MODIS) (Platnick *et al.*, 2003) are used to show the relationship of cloud properties to precipitation rate in the tropics. KHW consider clouds with tops colder than 245K and divide them into groups according to the optical depth. This temperature corresponds to a relative minimum in the distribution of cloud top temperature measured by MODIS. Two optical depth cutoffs were chosen. An optical depth (τ) of 4 approximately separates thin clouds with a positive net cloud radiative forcing from thicker clouds that cause a net reduction in the radiation balance at the top of the atmosphere. KHW defined cold clouds with $\tau < 4$ as thin clouds, cold clouds with $4 < \tau < 32$ to be anvil clouds, and cold clouds with $\tau > 32$ to be thick clouds. KHW found that thick clouds thus defined have a relationship with AMSR precipitation that is the same in the East Pacific and West Pacific (EP and WP), while anvil and thin clouds have a very different relationship with precipitation in the EP and WP. High optical depth clouds ($\tau>32$) are relatively rare in the MODIS observations, but they are an excellent marker for the deep convective cores that initiate much of the precipitation. Here we use these same definitions of thin, anvil and thick clouds to test the relationship of clouds to precipitation in a cloud-resolving model. The partitioning of cloud types by optical depth is a simplification of previous ISCCP categorizations (Chen *et al.*, 2000: Rossow *et al.*, 2005), but the separation into warming, cooling and heavily precipitating cold clouds is a physically motivated and objective basis for comparing models with data in a way that relates cloud morphology to cloud radiative effects.

The satellite data comes from the Aqua MODIS Joint Level-2 Dataset, containing information about cloud fraction, optical depth, and cloud top temperature. These fields are used to determine fractions of each cloud type in 1-degree by 1-degree regions, averaged over a 3 day time scale. For each datum, a corresponding rain rate is obtained from the AMSR collocated on the Aqua Satellite. All observations are made at 1:30 p.m. local time. See Kubar et al. (2007) for more detailed discussion of the satellite methodology.

3. Three-Dimensional Modeling Methodology

We employ the System for Atmospheric Modeling (SAM) version 6.3, a three dimensional CRM developed at Colorado State University (Khairoutdinov and Randall, 2003). The 3-D SAM simulations are set up in a similar manner to those in Blossey et al. (2007). We use a horizontal domain of 256 by 256 km with 1 km resolution. The model has 64 levels in the vertical. Spacing between levels varies from 75 m at the surface to 400 m through most of the troposphere and finally 1 km in the "sponge region" (top 30% of domain). The purpose of the sponge region is to prevent upward propagating gravity waves from bouncing off the top of the model and traveling downward. To represent near equatorial conditions, the Coriolis parameter is set to zero. The model does not use a planetary boundary layer scheme apart from enhanced vertical resolution near the surface and skin friction. Also, an ocean mixed layer is not included, since the SST is specified. The model utilizes a Smagorinsky scheme for subgrid scale turbulent transport and the radiation scheme from CAM 3.0. Insolation is constant with the diurnal average

zenith angle and irradiance. A nominal 6 second time step is used. Radiation is computed every 6 minutes.

The prognostic thermodynamic variables in SAM are non-precipitating water, precipitating water, and liquid/ice moist static energy. Non-precipitating water includes water vapor, cloud liquid, and cloud ice, while precipitating water includes rain, snow, and graupel. Partitioning between hydrometeor species is based on temperature. Supersaturation of water vapor is not allowed. In the CAM 3.0 radiation scheme, water vapor, cloud liquid, and cloud ice are all radiatively active, but precipitating hydrometeors are not. The default one-moment bulk microphysical parameterization of SAM is used (Appendix D of Khairoutdinov and Randall (2003)), except that cloud ice fall speed is calculated as a function of ice water content following Heymsfield (2003), replacing the default parameterization in which cloud ice fall speed is fixed at a constant value of 40 cm s^{-1}.

An idealized profile of zonal wind is specified, decreasing linearly from 5 m/s at the surface to zero at the tropopause in both runs, and zonal winds are nudged to these prescribed values on a 2-hour time scale. This shear profile was chosen to be weak yet inhibit domain-scale self-aggregation of convection (Bretherton *et al.*, 2005).

We wish to compare satellite observations with a cloud-resolving model simulation. In order for this to be useful, we must set up the model in such a way that we might expect it to produce the observed cloud statistics. We do this by running the model to equilibrium in the presence of the large-scale forcing that we believe was active in the time and place that the observations were taken. Convectively active regions of the Tropical East Pacific (EP: 7.5-10N, 140-120W) and West Pacific (WP: 5-7.5N, 140-

160E) are selected. Large-scale forcing is applied to the simulation by imposing the temperature and moisture forcing consistent with vertical advection of the large-scale vertical velocity profiles derived by Back and Bretherton (2006) from reanalysis data (Fig. 1). Qualitatively, these profiles are described as "bottom heavy" in the East Pacific and "top heavy" in the West Pacific. Each profile has been normalized in amplitude to produce a domain-mean rainfall rate of approximately 15 mm/day. Differences between the clouds in the simulations are thus due to the profile shape, not the overall domain-mean intensity of convection. SST is fixed at 302.49 K in both simulations to further assure that differences between the two simulations are a result of the imposed vertical motion profiles, rather than differences in SST.

The simulations are run for a total of 10 days, after having been run on a smaller 64 by 64 km domain for 50 days to a state of radiative convective equilibrium (RCE). Instantaneous fields are output every hour. The final 9 days when the 256x256 km model has equilibrated are used to gather the cloud and precipitation statistics for comparison with the observations. Because thin, anvil and thick cloud fractions are not model output variables, they are calculated from the instantaneous model data, using a column-by-column algorithm. In each layer of every column, visible optical depth is calculated using liquid/ice water path and effective radius:

$$\tau_{layer} = \frac{3}{2}\frac{LWP}{r_{el}} + \frac{3}{2}\frac{IWP}{r_{ei}}, \qquad (1)$$

where liquid water path (LWP) and ice water path (IWP) are in g m^{-2}, and r_{el} and r_{ei} are the effective radii for liquid and ice clouds in microns. The effective radius for cloud liquid water is 14 microns. For cloud ice, effective radius varies from ~6 microns at

temperatures below 180 K to ~250 microns at temperatures above 274 K, using a lookup table. These are the same specifications used in the radiative transfer model in the simulations. Total column visible optical depth is then calculated as the cumulative sum of the optical depth in every layer of the column.

Because we desire to determine cloud top temperature using a technique similar to that of the satellite observations with which we will compare the model, cloud top temperature, T_C, for the column is determined as the temperature at the top of the layer where cumulative optical depth from TOA exceeds 0.1, which is the minimal optical depth requirement that we impose for the column to contain a cloud. Clouds are classified as high, if $T_c < 245^{\circ}K$. Cloud fractions for the cold cloud types defined by KHW are determined for blocks of 64 by 64 km, which is approximately the size of the blocks in the satellite data.

We examine cloud fraction as a function of rain rate. Rain rate is directly related to the latent heating term that drives the tropical circulation, and the relationship between rain rate and cloud amount is a fundamental quantity of importance for climate. For each block, mean rain rate is obtained by averaging the surface rain rate of all the columns within the block. Using hourly output fields, an aggregate of cloud fractions and mean rain rates is formed. Percentiles of rain rate are calculated from the mean rain rates, ignoring mean rain rates less than 0.1 mm/day so that the percentiles will better resolve the larger rain rates. We next bin cloud fraction by percentile of rain rate to obtain a relationship between average cloud fraction and rain rate as in KHW.

4. Three-Dimensional Results

Fig. 2 shows the cloud amounts for the EP and WP regions as a function of rain rate for both the 3-D model simulations and for the satellite observations. The bottom panel shows the relationship of thick cloud (T_c<245K, τ>32) fraction to precipitation rate. The model and the observations fall nearly on the same lines in both the EP and WP regions. The middle panel shows the relationship of anvil cloud fraction (T_c <245K, 4<τ<32) to precipitation rate. In this case the model shows far too little anvil cloud and the anvil cloud amount does not increase with precipitation rate as observed. The top panel shows the thin cloud (T_c <245K, τ<4) fraction as a function of rain rate. The thin cloud amounts are close to those observed, the weak dependence on precipitation rate is simulated, and the much larger thin cloud amount in the WP than the EP is also well simulated. These results suggest that the thin clouds in both the model and the observations are not uniquely related to the amount of anvil cloud. Animations of the model simulation suggest that the thin cloud is not connected directly to the anvil cloud, but rather seems to be a result of the uniform cooling imposed at high levels, especially in the WP (Fig. 1).

Thin cloud fraction is somewhat independent of rain rate in both the East and West Pacific simulations, but a decrease in thin cloud fraction occurs at the highest rain rates. This decrease at high rain rates is probably due to convective cores and anvils being the dominant cloud species in places where precipitation is most intense, thus decreasing the space available within the 1˚x1˚ box for thin cloud.

Because the cloud fraction versus rain rate composites only convey information about cloud amount in places where precipitation is occurring, it is possible that our methodology fails to detect some anvil clouds, if they spread to regions where precipitation is extremely light (less that 0.1 mm/day). To eliminate this as a possibility, we examine domain average cloud fraction.

Table 1 shows domain average comparisons between the SAM model simulation and the satellite observations for the EP and WP regions derived from MODIS temperature-optical depth histograms. The domain average rain rates are higher in the model because it shows very high rain rates that are not present in the observations. Although the rain rate in the model is greater than that in the observations, and correspondingly more thick cloud is present, the anvil cloud fraction is much smaller than observed, confirming that the 3-D simulations do not produce enough anvil cloud. Domain average high thick cloud fraction agrees reasonably well with observations, as suggested by the composites with rain rate in Fig. 2. Domain average high thin cloud fraction is slightly higher than observations in the East Pacific and nearly agrees with observations in the West Pacific. Although the rain rate composites suggest that the model over-produces high thin cloud in the West Pacific, the unexpected agreement with observations in Table 1 may indicate that high thin clouds in the West Pacific are abundant in non-raining regions, perhaps sustained by gravity waves or the mean rising motion in the upper troposphere. Because domain average rain rate in the simulations is significantly larger than the AMSR observations, the amount of cold cloud per unit of precipitation in the model is actually quite low compared to AMSR/MODIS observations.

Table 1 shows that the anvil to thick cloud fraction in the observations is 5.2-6.6, but in the model is 1.4-1.8.

Table 1 shows large biases in the domain-mean albedo, with the model albedo around 0.25 and the observed albedo nearly 0.4 in both regions. The model OLR is too high by 20Wm^{-2} in the EP and nearly 40 Wm^{-2} too high in the WP. The model does show a higher OLR in the EP by about 20 Wm^{-2}, compared to the observed EP-WP difference of 37 Wm^{-2}. The OLR discrepancy is fractionally less than the albedo discrepancy because the model produces high, thin clouds in close to the observed abundance, which are important for the OLR, but produces far too little extended upper level cloud of intermediate optical depths (anvil clouds), which are more important for the albedo.

To further investigate how the lack of anvil clouds significantly affects the TOA energy budget, we examine PDFs of albedo and OLR. The PDFs are constructed from values of albedo and OLR at every point in the domain of the model as well as in the corresponding observational domain. To construct PDFs from the observations, the radiative transfer model of Fu and Liou (1993) is used to calculate albedo and OLR in the domain of the observations, based upon the MODIS observed cloud property histogram. The cloud properties used in the radiative transfer calculations are based upon pixel level MODIS data (5x5 km), so that they can be directly comparable to the grid point level PDFs obtained from the model. Temperature and humidity profiles from the Atmospheric Infrared Sounder (AIRS) Version 2 data from Jan. 2003 to Dec. 2005 are used in the calculations (Aumann *et al.*, 2003).

In the observations, the PDF of albedo has two modes (Fig. 3). The first mode, centered near 0.1, corresponds to nearly clear skies. The second mode is weak peak around 0.7, corresponding to optically thick clouds that are tropical anvil cloud structures and associated convective cores. In the simulations, the clear-sky mode is more prevalent, the PDF of albedo decays rapidly toward higher albedos, and high albedo mode is absent. The model PDFs of OLR show discrepancies that are consistent with the albedo (Fig.4). Observations show one mode at high OLR corresponding to clear skies and another mode at about 120 Wm^{-2}, corresponding to the modal anvil cloud top temperature. The model OLR PDF has a broad peak near the clear-sky value and does not show the observed peak at low OLR values that is associated with anvil clouds. The clear-sky peak in the model also occurs at a lower value of OLR than the PDF calculated from the MODIS/AIRS data. This may be associated with the strong forcing of the model with the velocity profiles in Fig. 1 and the correspondingly moist profiles and high water vapor path in the simulations.

5. Two-Dimensional Mock-Walker Simulations

In this section we consider 2-D calculations using the SAM model to see if the relationship between precipitation amount and upper level cloud amounts is different in two dimensions and under the condition where we allow a large-scale circulation to develop in the domain, rather than specifying the circulation externally. We find that the 2-D Mock-Walker circulation experiments produce similar relationships between anvil clouds and precipitation as the three-dimensional simulations just described. We then use the 2-D model to test the sensitivity of the cloud simulations to changes in the cloud

physical parameterizations and other model details. Two-dimensional simulations require less computer resources, and thereby allow easier testing of sensitivity to model parameters.

We begin by examining a base case (BASE), a two dimensional SAM simulation like that described in Bretherton et al. (2006), which uses horizontal domain size and grid resolution of 4096 km and 2 km, respectively. SST is fixed as a sinusoidal function of distance, creating a warm pool in the center of the domain with a maximum temperature of 301˚K and a minimum temperature of 297˚K. The atmosphere organizes into an overturning circulation with convection and upward motion mainly confined to the warm water (Grabowski *et al.*, 2000: Bretherton *et al.*, 2006). Vertical resolution and the parameterizations for microphysics, radiation, and sub-grid turbulent transport remain the same as in the 3-D runs. Again, the insolation has no diurnal cycle. Although we do not apply large-scale forcing to the atmosphere directly, a large-scale circulation develops in response to the imposed SST gradient, allowing us to examine how high cloud properties depend upon precipitation rate in a less constrained environment than was used for the 3-D simulations. Domain-mean winds are nudged to zero on a 2 hour time scale to prevent the development of mean shear unrelated to the Walker circulation.

The 2-D model is run for a total of 50 days and data are taken every three hours for the last 20 days of the integration. The same column-by-column algorithm from the 3-D runs is used to determine the abundance of thin, anvil, and thick clouds. A larger horizontal averaging block size of 128 km is used for the 2-D model in order to provide better sampling, and averages are taken over three adjacent time samples.

BASE has too little anvil cloud amount per unit of precipitation to roughly the same degree as the 3-D runs (dotted line in Fig. 2), and the ratio of anvil cloud to thick cloud in BASE is 1.4, very similar to the 3-D EP case, and far less than observed. Anvil cloud fraction seems to be more strongly dependent on rain rate than in the 3-D runs, however, and anvil cloud fraction approaches 20% at the highest rain rate, compared to 40% in the observations. The thick cloud amount increases more quickly with rain rate than observed, however. For rain rates less than 10 mm/day, thin cloud fraction is noticeably less than in the observations. In the 2-D runs the mean vertical velocity is determined internally to the model at all locations.

6. Parameter Variations in 2-D Mock-Walker Simulation.

Because BASE under-produces anvil cloud by roughly the same degree as the 3-D runs, we use the mock-Walker simulation as a tool for testing the sensitivity of anvil cloud in SAM to adjustments to the physics and resolution of the model. In this spirit, a suite of 2-D mock-Walker simulation experiments is performed using different adjustments to BASE, involving microphysics, resolution, and domain size. The 2-D experiments are summarized in Table 2. Microphysics experiments include reduction of cloud ice fall speed, decreased and increased rates of autoconversion and accretion, and elimination of graupel formation. In horizontal resolution experiments, resolution is increased from the default value of 2 km to 1 km and 0.5 km. Vertical resolution experiments use an increased number of levels in the ice cloud layer. Experiments are also conducted with the domain size doubled to 8192 km, twice as large as in BASE.

a. Microphysics

Changes to microphysics may be a plausible way to increase anvil cloud amount, because microphysical processes play a critical role in determining the amount of ice in the atmosphere. Krueger et al. (1995) used microphysical adjustments to increase the extent and ice water content of tropical anvil clouds in a CRM, by making changes to parameterizations of cloud ice growth, snow formation, and graupel. Also, microphysical processes may affect atmospheric circulation. By removing cold cloud processes from a 2-D CRM, Grabowski (2003a: 2003b) showed that in the warm-rain only version of the model the mesoscale convective systems have a shorter life cycle and reduced stratiform component. In addition to direct effects on cloud formation and dissipation, cloud ice microphysics play an important role in determining mesoscale circulations that may be important to the dynamics of anvil clouds.

Cloud Ice Fall Speed

In the microphysical parameterizations of SAM, cloud ice is allowed to fall slowly, although it is considered to be a non-precipitating hydrometeor species. We expect that anvil cloud amount will increase if cloud ice fall speed is reduced. In these simulations cloud ice fall speed is parameterized as a function of ice water content, following Heymsfield (2003):

$$v_{t_{ice}} = 165(IWC)^{0.24}, \tag{2}$$

with $v_{t_{ice}}$ in cm/s and IWC in g/m^3. In VTHALF, the cloud ice fall speed computed in the preceding formula is multiplied by one half.

VTHALF fails to improve the relationship between anvil cloud fraction and rain rate (Fig. 5). Although anvil cloud fraction increases noticeably, it becomes nearly independent of rain rate and is less than half the observed amount at the highest rain rates. Moreover, thick cloud fractions also increase in VTHALF, so that decreasing the ice fall speed increases the fractional coverage of all cloud types and does not improve the ratio of anvil cloud to thick cloud.

Autoconversion and Accretion

The rate of autoconversion determines how quickly cloud liquid or ice is converted to precipitation by coalescence or aggregation, respectively. By reducing this rate, the onset of precipitation may be delayed, potentially prolonging cloud lifetime. The accretion rate controls the growth of precipitating condensate through the collection of non-precipitating condensate. To examine the effect of changing the rates of autoconversion and accretion, AAHALF, AATWO and AATEN multiply the default rates of autoconversion and accretion for both liquid and ice by factors of 0.5, 2 and 10, respectively.

These experiments have little effect on anvil clouds. The relationship between anvil fraction and rain rate in AAHALF and AATWO is nearly identical to the relationship found in BASE (Fig. 5). AATEN is very similar to AATWO and is not shown. Interestingly, increasing the autoconversion rates as in AATWO reduces the thick cloud fractions so that they compare better with observations at all rain rates than BASE. Increased rates of autoconversion and accretion in AATWO increase precipitation efficiency in convective cores. As a result, high thick cloud fraction decreases because

cloud liquid water below the freezing level is rained out more readily. Consistent with this, AAHALF noticeably overproduces high thick clouds, a bias which becomes quite large at rain rates greater than 10 mm day^{-1}.

We also experimented with changing the autoconversion and accretion rates for ice only. The results of these experiments are indistinguishable from BASE, and so we conclude that the behavior of high cloud fraction witnessed in AAHALF and AATEN is due mostly to changes in the liquid autoconversion and accretion rates. Note that while we define high clouds by their cloud top temperature, their albedos are affected by the water and ice content over a deep layer.

Graupel

Graupel forms when ice particles accrete cloud liquid. If ice particles are precipitating inside convective cores, a significant amount of liquid water may be lost through the formation of graupel. The increase in graupel at the expense of cloud liquid within convective cores would seem to reduce the amount of water that can be lofted upward to higher levels where it could possibly detrain in the formation of anvil clouds. Therefore, reducing the amount of graupel in SAM may increase the amount of anvil clouds produced. NOGRAU eliminates graupel as a precipitating hydrometeor species.

NOGRAU does not improve the relationship between anvil cloud fraction and rain rate (not shown). Also, high thin cloud amount does not change substantially. It is somewhat surprising that high thick cloud fraction remains similar to BASE, because the lack of graupel suggests an increase in the amount of cloud liquid water inside convective

cores. Any changes in cloud water produced by the elimination of graupel seem to be offset by the other microphysical processes in the model.

Combinations of Cloud Physics Changes

So far we have determined that cloud physics parameters affect the amount of cloud, but we wish to find a combination of effects that increases the amount of moderate optical depth ice cloud and its dependence on rain rate, and also decreases the amount of liquid water cloud in the convective cores. In this section we describe a combination of cloud physics changes that achieves this result.

Another experiment (NOSED) was undertaken in which cloud ice sedimentation is set to zero and the cloud ice to snow autoconversion threshold is lowered from 1.0×10^{-4} kg kg^{-1} to 1.0×10^{-6} kg kg^{-1}. With these changes, the lack of cloud ice sedimentation is offset to some extent by the lower cloud ice autoconversion threshold. This combination of changes is found to produce TOA radiative fluxes closer to observed values in multiscale modeling framework GCM runs than the default SAM settings (Khairoutdinov, personal communication). Incorporating these changes in another 2-D experiment, we find a noticeable increase in the amount of high thin cloud and anvil cloud produced by SAM, and that the relationship between anvil cloud fraction and rain rate varies in a manner similar to the observations (Fig. 6). The amount of high thick cloud becomes excessive at high rain rates, however, as is the case in many of our previous 2-D experiments.

To reduce the amount of thick cloud, we set the ice sedimentation to zero and lower the threshold for autoconversion as in NOSED above, but we also increase the

rates of autoconversion and accretion for liquid water by factors of two and five (NOSEDAALIQ2 and NOSEDAALIQ5). The results of these experiments are shown in Fig. 6. The anvil cloud fraction is increased and it has the observed dependence on rain rate as in NOSED, but the amount of thick cloud is also decreased to be much more like the observed amounts, especially for NOSEDAALIQ5. We thus have succeeded in tuning the cloud physics parameters to produce a much better simulation of convective cloud optical depth as a function of rain rate. This tuning is not fundamental, as the parameters are not chosen for physical reasons and may be compensating for other errors in the model. Also, it is probable that this tuning is not unique, even within the context of this model. For example, results approaching those of NOSEDAALIQ5 can be obtained with a small uniform sedimentation velocity, rather than zero sedimentation and increased autoconversion, but the dependence on rain rate is not as good (not shown). Nonetheless, the model behavior is closer to that observed when the NOSEDAALIQ5 parameters are used. Later we will test to see if this tuning improves the 3-D simulation, but we will next look at the sensitivity to some other model parameters.

b. Spatial Resolution

Spatial resolution of the model may affect the physical processes important to anvil cloud formation. To investigate whether finer horizontal resolution than the default 2 km may increase anvil amount, we perform experiments HORRES 1 and HORRES 0.5 which use horizontal resolutions of 1 km and 0.5 km, respectively. Also, it is useful to investigate the sensitivity of anvil cloud amount to changes in the vertical resolution of

SAM. VERTRES increases vertical resolution by using 200 m spacing between levels throughout the ice cloud layer.

The experiments with higher horizontal and vertical resolution do not significantly affect the relationship between anvil cloud fraction and rain rate, or any of the cloud amounts (not shown). Pauluis and Garner (2006) found that increases in CRM resolution finer than 4km do not affect the amount of simulated high cloud.

c. Domain Size

A larger domain contains a more realistic SST gradient and gives convection more space to organize. BIG doubles the size of the horizontal domain to 8192 km, creating a warm pool twice as large as the one that exists when using the default domain size. Maximum and minimum SSTs and horizontal and vertical resolutions remain at their values used in BASE. The larger horizontal domain in BIG does not change anvil cloud amount significantly, and the amount of thick cloud is even more excessive than for the smaller domain (not shown). A series of experiments was performed with microphysical changes with the doubled domain, but these results are consistent with the microphysical testing described above and will not be discussed.

d. A 3-D test of tuned microphysical parameters

We performed a 3-D simulation (WP2) with the WP forcing in which the microphysical parameters from NOSEDAALIQ5 were employed. Some results for this case are shown in Table 3 and compared with the WP and EP experiments. The cloud liquid water path is greatly decreased by the new parameters, while the ice water path

remains about the same. Nonetheless, the SWCF is increased by about 40% because the ice water path is spread over a larger area in clouds with intermediate optical thickness, as we had hoped. Total water vapor path remains about the same, but the net flux into the ocean decreases by about 15 W m^{-2} in association with greater cloud reflection. Surface evaporative cooling decreases slightly and sensible cooling remains small. The LWCF nearly doubles from 48 to 93 W m^{-2}. In ERBE observations the LWCF and SWCF are of order 80 W m^{-2} and SWCF is about 10 W m^{-2} larger in magnitude than LWCF, so that the net cloud forcing is weakly negative. These numbers depend on what region and season is chosen for averaging. The cloud forcing for experiment WP2 is much closer to the observed values for the deep convective regions of the Tropics than WP, so that the change in cloud physical parameters suggested by the 2D experiments does produce an improvement in the simulation of the radiative effects of tropical cloud complexes in the 3D model.

Other aspects of the WP2 simulation are not so good, however. Thin cloud nearly fills the model domain at upper levels, so that the cloud fraction is near 90%. The histograms of albedo and OLR no longer have clear sky maxima as in observations or previous model results (not shown). This is because the imposed cooling at upper levels continuously cools the temperature toward saturation and the resulting clouds fill the 256 km domain used in the calculations. Because of the limitations of the three dimensional methodology employed here we have chosen not to pursue an optimal set of cloud physical parameters for these simulations.

7. Conclusion

We have introduced metrics for using satellite data to test the simulation of tropical convection by a cloud-resolving model. Upper level cloudiness is divided into categories corresponding to thin cloud, anvil cloud and deep convective cores that are closely related to precipitation rate. These three categories are chosen to succinctly characterize the relationships among precipitation, cloud structure and the TOA radiation balance, and to allow easy comparison with satellite data.

In testing 3-D and 2-D simulations with the SAM model, we have found that the default model parameters give too little anvil cloud per unit of precipitation, although thin clouds and thick clouds are in much better accord with observations. For the default parameters, anvil clouds are not abundant enough and do not show the observed increase with precipitation rate. The PDFs of OLR and albedo for the default simulation do not show the features that are associated with tropical anvil clouds; a peak in the OLR PDF associated with the anvil cloud top temperature and a broad distribution of high albedos. Our results are in general agreement with the experiments of Blossey et al. (2007) attempting to simulate the KWAJEX data.

The cloud ice can easily be increased by decreasing the ice fall speed, but this increases all cold cloud amounts, leading to an over-prediction of thin and thick clouds, and does not improve the ratio of anvil to thick clouds. To produce a cloud albedo distribution like that observed, simultaneous changes of several parameters are necessary. Decreasing the fall speed of ice while simultaneously increasing the liquid water accretion rates can lead to an improvement in the ratio of anvil to thick clouds. Setting the ice fall speed to zero while lowering the threshold for ice accretion increases the

amount of anvil cloud and improves its dependence on rain rate, but also increases the amount of thick cloud, so that the ratio of anvil to thick cloud is still imperfect. Adding increased rates of autoconversion and accretion for liquid water to a simulation in which the ice fall speed is set to zero and the autoconversion threshold is lowered gives dependences of thick, anvil and thin clouds on rain rate in the 2-D model that are in reasonable agreement with observations. The results are not very sensitive to a factor of 4 change in model resolution. It is unclear to what extent the changes in bulk microphysical parameters are justified on physical grounds, or rather are compensating for other errors in the model microphysics or dynamics in order to produce clouds that have characteristics more like those of observed clouds.

Acknowledgments. This work was supported by NSF Grant ATM 04-09075, NASA Grant NNG05GA19G and NOAA grant NA06OAR4310055. Marat Khairoutdinhov kindly made SAM available to us at UW. Mark Zelinka provided averaged AIRS profiles for the EP and WP regions and Marc Michelsen provided computer expertise.

REFERENCES

Aumann, H. H., M. T. Chahine, C. Gautier, M. D. Goldberg, E. Kalnay, L. M. McMillin, H. Revercomb, P. W. Rosenkranz, W. L. Smith, D. H. Staelin, L. L. Strow, and J. Susskind, 2003: AIRS/AMSU/HSB on the aqua mission: Design, science objectives, data products, and processing systems. *IEEE Trans. Geo. Rem. Sens.*, **41,** 253-264.

Back, L. E. and C. S. Bretherton, 2006: Geographic variability in the export of moist static energy and vertical motion profiles in the tropical Pacific. *Geophys. Res. Lett.*, **33,** doi:10.1029/2006GL026672.

Blossey, P. N., C. S. Bretherton, J. Cetrone, and M. Khairoutdinov, 2007: Cloud-resolving model simulations of KWAJEX: Model sensitivities and comparisons with satellite and radar observations. *J. Atmos. Sci.*, **64,** 1488–1508.

Bony, S., R. Colman, V. M. Kattsov, R. P. Allan, C. S. Bretherton, J. L. Dufresne, A. Hall, S. Hallegatte, M. M. Holland, W. Ingram, D. A. Randall, B. J. Soden, G. Tselioudis, and M. J. Webb, 2006: How well do we understand and evaluate climate change feedback processes? *J. Climate*, **19,** 3445-3482.

Bretherton, C. S., P. N. Blossey, and M. Khairoutdinov, 2005: An energy-balance analysis of deep convective self-aggregation above uniform SST. *J. Atmos. Sci.*, **62,** 4273-4292.

Bretherton, C. S., P. N. Blossey, and M. E. Peters, 2006: Interpretation of simple and cloud-resolving simulations of moist convection-radiation interaction with a mock-Walker circulation. *Theor. Comp. Fluid Dyn.*, **20,** 421-442.

Chambers, L. H., B. Lin, and D. F. Young, 2002: Examination of new CERES data for evidence of tropical Iris feedback. *J. Climate*, **15,** 3719-3726.

Chen, S. S., R. A. Houze, Jr., and B. E. Mapes, 1996: Multiscale variability of deep convection in relation to large- scale circulation in TOGA COARE. *J. Atmos. Sci*., **53,** 1380-1409.

Chen, T., W. B. Rossow, and Y. C. Zhang, 2000: Radiative effects of cloud-type variations. *J. Climate*, **13,** 264-286.

Comstock, J. M. and C. Jakob, 2004: Evaluation of tropical cirrus cloud properties derived from ECMWF model output and ground based measurements over Nauru Island. *Geophys. Res. Lett.*, **31,** doi:10.1029/2004GL019539.

Del Genio, A. D. and W. Kovari, 2002: Climatic properties of tropical precipitating convection under varying environmental conditions. *J. Climate*, **15,** 2597-2615.

Del Genio, A. D., W. Kovari, M. S. Yao, and J. Jonas, 2005: Cumulus microphysics and climate sensitivity. *J. Climate*, **18,** 2376-2387.

Donner, L. J., C. J. Seman, R. S. Hemler, and S. M. Fan, 2001: A cumulus parameterization including mass fluxes, convective vertical velocities, and mesoscale effects: Thermodynamic and hydrological aspects in a general circulation model. *J. Climate*, **14,** 3444-3463.

Eitzen, Z. A. and K. M. Xu, 2005: A statistical comparison of deep convective cloud objects observed by an Earth Observing System satellite and simulated by a cloud-resolving model. *J. Geophys. Res. Atmos.*, **110,** doi:10.1029/2004JD005086.

Fu, Q. and K. N. Liou, 1993: Parameterization of the radiative properties of cirrus clouds. *J. Atmos. Sci.*, **50,** 2008-2025.

Fu, Q., M. Baker, and D. L. Hartmann, 2002: Tropical cirrus and water vapor: an effective Earth infrared iris feedback? *Atmos. Chem. Phys.*, **2,** 31-37.

Fu, R., A. D. Del Genio, W. B. Rossow, and W. T. Liu, 1992: Cirrus-cloud thermostat for tropical sea surface temperatures tested using satellite data. *Nature*, **358,** 394-397.

Grabowski, W. W., 2001: Coupling cloud processes with the large-scale dynamics using the Cloud-Resolving Convection Parameterization (CRCP). *J. Atmos. Sci.*, **58 (9),** 978-997.

——, 2003a: Impact of ice microphysics on multiscale organization of tropical convection in two-dimensional cloud-resolving simulations. *Quart. J. Roy. Meteor. Soc.*, **129,** 67-81.

——, 2003b: Impact of cloud microphysics on convective-radiative quasi equilibrium revealed by cloud-resolving convection parameterization. *J. Climate*, **16,** 3463-3475.

——, 2003c: MJO-like coherent structures: Sensitivity simulations using the cloud-resolving convection parameterization (CRCP). *J. Atmos. Sci.*, **60,** 847-864.

Grabowski, W. W., J. I. Yano, and M. W. Moncrieff, 2000: Cloud resolving modeling of tropical circulations driven by large-scale SST gradients. *J. Atmos. Sci.*, **57,** 2022-2039.

Hartmann, D. L. and M. L. Michelsen, 1993: Large-scale effects on the regulation of tropical sea surface temperature. *J. Climate*, **6,** 2049-2062.

——, 2002: No Evidence for Iris. *Bull. Amer. Meteor. Soc.*, **83,** 249-254.

Hartmann, D. L. and K. Larson, 2002: An important constraint on tropical cloud - climate feedback. *Geophys. Res Lett.*, **29(20),** doi:10.1029/2002GL015835.

Hartmann, D. L., H. H. Hendon, and R. A. Houze, 1982: Some implications of the mesoscale circulations in tropical cloud clusters for large-scale dynamics and climate. *J. Atmos. Sci.*, **41,** 113-121.

Hartmann, D. L., M. E. Ockert-Bell, and M. L. Michelsen, 1992: The effect of cloud type on Earth's energy balance: global analysis. *J. Climate,* **5,** 1281-1304.

Hartmann, D. L., L. A. Moy, and Q. Fu, 2001: Tropical convection and the energy balance at the top of the atmosphere. *J. Climate*, **14,** 4495-4511.

Heymsfield, A. J., 2003: Properties of tropical and midlatitude ice cloud particle ensembles. Part II: Applications for mesoscale and climate models. *J. Atmos. Sci.*, **60,** 2592-2611.

Houze, R. A., 1982: Cloud clusters and large-scale vertical motions in the tropics. *J. Meteor. Soc. Japan,* **60,** 396-410.

IPCC, 2007: *Climate Change 2007: The Physical Science Basis*. Cambridge University Press, 800 pp.

Khairoutdinov, M. F. and D. A. Randall, 2003: Cloud resolving modeling of the ARM summer 1997 IOP: Model formulation, results, uncertainties, and sensitivities. *J. Atmos. Sci.*, **60,** 607-625.

Krueger, S. K., Q. A. Fu, K. N. Liou, and H. N. S. Chin, 1995: Improvements of an Ice-Phase Microphysics Parameterization for Use in Numerical Simulations of Tropical Convection. *J. Appl. Meteorol.*, **34,** 281-287.

Kuang, Z. and D. L. Hartmann, 2007: Testing the Fixed Anvil Temperature Hypothesis in a Cloud-Resolving Model *J. Climate*, **20,** 2051-2057.

Kubar, T. L., D. L. Hartmann, and R. Wood, 2007: Radiative and Convective Driving of Tropical High Clouds. *J. Climate***,** in press.

Lau, K.-M., C.-H. Sui, M.-D. Chou, and W.-K. Tao, 1994: An inquiry into the cirrus-cloud thermostat effect for tropical sea-surface temperature. *Geophys. Res. Lett.*, **21,** 1157-1160.

Leary, C. A. and R. A. Houze, 1980: The Contribution of Mesoscale Motions to the Mass and Heat Fluxes of an Intense Tropical Convective System. *J. Atmos. Sci.*, **37,** 784-796.

Li, J. L., D. E. Waliser, J. H. Jiang, D. L. Wu, W. Read, J. W. Waters, A. M. Tompkins, L. J. Donner, J. D. Chern, W. K. Tao, R. Atlas, Y. Gu, K. N. Liou, A. Del Genio, M. Khairoutdinov, and A. Gettelman, 2005: Comparisons of EOS MLS cloud ice measurements with ECMWF analyses and GCM simulations: Initial results. *Geophys. Res. Lett.*, **32,** doi:10.1029/2005GL023788.

Lin, B., T. M. Wong, B. A. Wielicki, and Y. X. Hu, 2004a: Examination of the decadal tropical mean ERBS nonscanner radiation data for the iris hypothesis. *J. Climate*, **17,** 1239-1246.

Lin, B., B. A. Wielicki, L. H. Chambers, Y. X. Hu, and K. M. Xu, 2002: The iris hypothesis: A negative or positive cloud feedback? *J. Climate*, **15,** 3-7.

Lin, B., B. A. Wielicki, P. Minnis, L. Chambers, K. M. Xu, Y. X. Hu, and A. Fan, 2006: The effect of environmental conditions on tropical deep convective systems observed from the TRMM satellite. *J. Climate*, **19,** 5745-5761.

Lin, J. L., B. Mapes, M. H. Zhang, and M. Newman, 2004b: Stratiform precipitation, vertical heating profiles, and the Madden-Julian oscillation. *J. Atmos. Sci.*, **61,** 296-309.

Lindzen, R. S., M. D. Chou, and A. Y. Hou, 2001: Does the earth have an adaptive infrared iris? *Bull. Amer. Meteorol. Soc.*, **82,** 417-432.

Luo, Y. L., S. K. Krueger, and S. Moorthi, 2005: Cloud properties simulated by a single-column model. Part I: Comparison to cloud radar observations of cirrus clouds. *J. Atmos. Sci.*, **62,** 1428-1445.

Luo, Y. L., K. M. Xu, B. A. Wielicki, T. Wong, and Z. A. Eitzen, 2007: Statistical analyses of satellite cloud object data from CERES. Part III: Comparison with cloud-resolving model simulations of tropical convective clouds. *J. Atmos. Sci.*, **64,** 762-785.

Mapes, B., S. Tulich, J. Lin, and P. Zuidema, 2006: The mesoscale convection life cycle: Building block or prototype for large-scale tropical waves? *Dyn. Atmos. Oceans*, **42,** 3-29.

Mapes, B. E. and R. A. Houze, 1993: Cloud Clusters and Superclusters over the Oceanic Warm Pool. *Mon. Wea. Rev.*, **121,** 1398-1415.

Miura, H., H. Tomita, T. Nasuno, S. Iga, M. Satoh, and T. Matsuno, 2005: A climate sensitivity test using a global cloud resolving model under an aqua planet condition. *Geophys. Res. Lett.*, **32,** doi:10.1029/2005GL023672.

Ovtchinnikov, M., T. Ackerman, R. Marchand, and M. Khairoutdinov, 2006: Evaluation of the multiscale modeling framework using data from the atmospheric radiation measurement program. *J. Climate*, **19,** 1716-1729.

Pauluis, O. and S. Garner, 2006: Sensitivity of radiative-convective equilibrium simulations to horizontal resolution. *J. Atmos. Sci.*, **63,** 1910-1923.

Platnick, S., M. D. King, S. A. Ackerman, W. P. Menzel, B. A. Baum, J. C. Riedi, and R. A. Frey, 2003: The MODIS cloud products: Algorithms and examples from Terra. *IEEE Trans. Geosci. Rem. Sens.*, **41,** 459-473.

Ramanathan, V. and W. Collins, 1991: Thermodynamic regulation of ocean warming by cirrus clouds deduced from observations of the 1987 El Nino. *Nature*, **351,** 27-32.

Randall, D., M. Khairoutdinov, A. Arakawa, and W. Grabowski, 2003a: Breaking the cloud parameterization deadlock. *Bull. Amer. Meteorol. Soc.*, **84,** 1547-1564.

Randall, D., S. Krueger, C. Bretherton, J. Curry, P. Duynkerke, M. Moncrieff, B. Ryan, D. Starr, M. Miller, W. Rossow, G. Tselioudis, and B. Wielicki, 2003b: Confronting models with data - The GEWEX cloud systems study. *Bull. Amer. Meteorol. Soc.*, **84,** 455-469.

Rapp, A. D., C. Kummerow, W. Berg, and B. Griffith, 2005: An evaluation of the proposed mechanism of the adaptive infrared iris hypothesis using TRMM VIRS and PR measurements. *J. Climate*, **18,** 4185-4194.

Ringer, M. A. and R. P. Allan, 2004: Evaluating climate model simulations of tropical cloud. *Tellus A*, **56,** 308-327.

Rossow, W. B., G. Tselioudis, A. Polak, and C. Jakob, 2005: Tropical climate described as a distribution of weather states indicated by distinct mesoscale cloud property mixtures. *Geophys. Res. Lett.*, **32,** doi:10.1029/2005GL024584.

Schumacher, C., R. A. Houze, and I. Kraucunas, 2004: The tropical dynamical response to latent heating estimates derived from the TRMM precipitation radar. *J. Atmos. Sci.*, **61,** 1341-1358.

Stephens, G. L., 2005: Cloud feedbacks in the climate system: A critical review. *J. Climate*, **18,** 237-273.

Su, H., C. S. Bretherton, and S. S. Chen, 2000: Self-aggregation and large-scale control of tropical deep convection: A modeling study. *J. Atmos. Sci.*, **57,** 1797-1816.

Tompkins, A. M. and G. C. Craig, 1998: Radiative-convective equilibrium in a three-dimensional cloud-ensemble model. *Quart. J. Roy. Meteor. Soc.*, **124,** 2073-2097.

Wilheit, T., C. D. Kummerow, and R. Ferraro, 2003: Rainfall algorithms for AMSR-E. *IEEE Trans. Geosci. Rem. Sens.*, **41,** 204-214.

Wyant, M. C., M. Khairoutdinov, and C. S. Bretherton, 2006a: Climate sensitivity and cloud response of a GCM with a superparameterization. *Geophys. Res. Lett.*, **33,** doi:10.1029/2005GL025464.

Wyant, M. C., C. S. Bretherton, J. T. Bacmeister, J. T. Kiehl, I. M. Held, M. Zhao, S. A. Klein, and B. J. Soden, 2006b: A comparison of low-latitude cloud properties and their response to climate change in three AGCMs sorted into regimes using mid-tropospheric vertical velocity. *Clim. Dyn.*, **27,** 261-279.

Xu, K. M., T. Wong, B. A. Wielicki, L. Parker, B. Lin, Z. A. Eitzen, and M. Branson, 2007: Statistical analyses of satellite cloud object data from CERES. Part II: Tropical convective cloud objects during 1998 El Nino and evidence for supporting the fixed anvil temperature hypothesis. *J. Climate*, **20,** 819-842.

FIGURE CAPTIONS

Fig. 1. Profiles of vertical motion in West and East Pacific regions used to force the 3-D simulations.

Fig. 2. Average cloud fraction as a function of precipitation rate percentiles for EP (dashed) and WP (solid) regions from observations (thick lines), from the 3-D SAM model for the EP and WP regions (thin lines), and from the BASE simulation of the 2-D SAM model (dotted thin line). The top panel shows fractional coverage of optically thin, cold cloud ($T<245K$, $\tau<4$), the middle panel shows fractional coverage of anvil clouds ($T<245K$, $4<\tau<32$), and the bottom panel shows fractional coverage of thick cloud (($T<245K$, $\tau>32$).

Fig. 3 PDF of albedo for the observations and for the 3-D simulations for the EP and WP regions. Line conventions are as in Fig. 2.

Fig. 4 PDF of OLR, otherwise as in Fig. 3.

Fig. 5 As in Fig. 2, except that the thin lines are for the 2-D simulations BASE, VTHALF, AAHALF and AATWO. Heavy lines again represent observations for the EP and WP.

Fig. 6 As in Fig. 2, except that the thin lines are for the 2-D simulations NOSED, NOSEDAALIQ2, and NOSEDAALIQ5. Heavy lines again represent observations for the EP and WP.

FIGURES

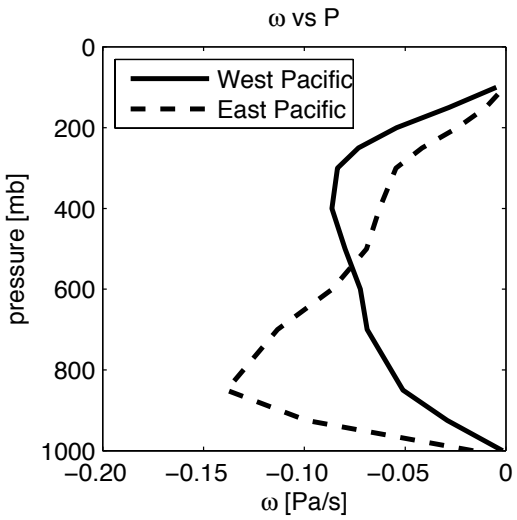

Fig. 1. Profiles of vertical motion in West and East Pacific regions used to force the 3-D simulations.

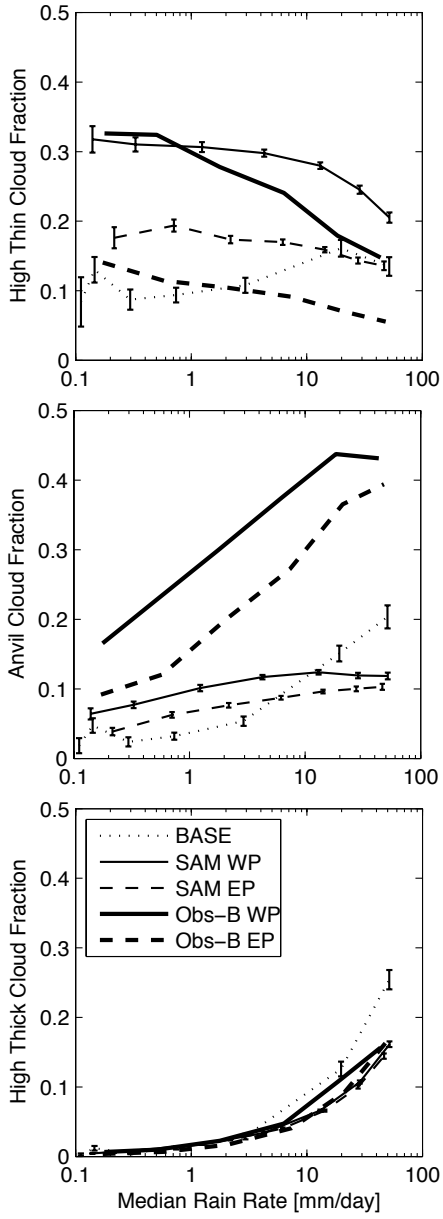

EP Fig. 2. Average cloud fraction as a function of precipitation rate percentiles for EP (dashed) and WP (solid) regions from observations (thick lines), from the 3-D SAM model for the EP and WP regions (thin lines), and from the BASE simulation of the 2-D SAM model (dotted thin line). The top panel shows fractional coverage of optically thin, cold cloud ($T<245K$, $\tau<4$), the middle panel shows fractional coverage of anvil clouds ($T<245K$, $4<\tau<32$), and the bottom panel shows fractional coverage of thick cloud (($T<245K$, $\tau>32$).

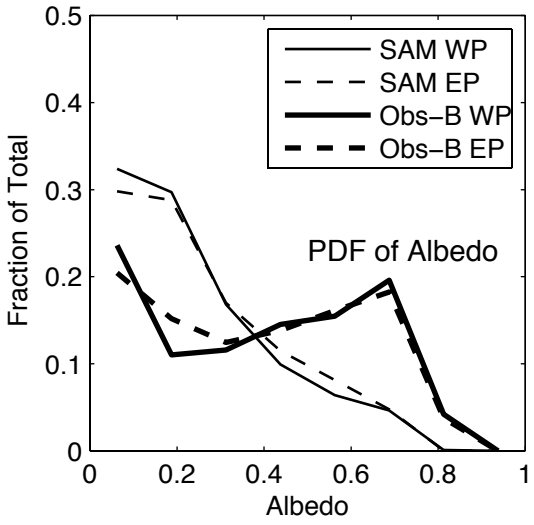

Fig. 3 PDF of albedo for the MODIS/AIRS observations and for the 3-D simulations for the EP and WP regions. Line conventions are as in Fig. 2.

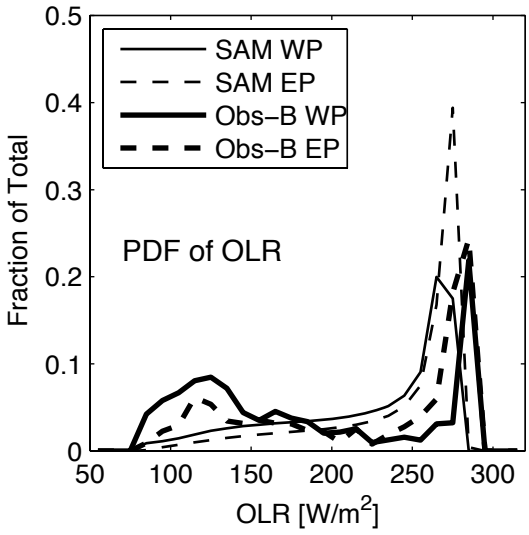

Fig. 4 PDF of OLR as in Fig. 3.

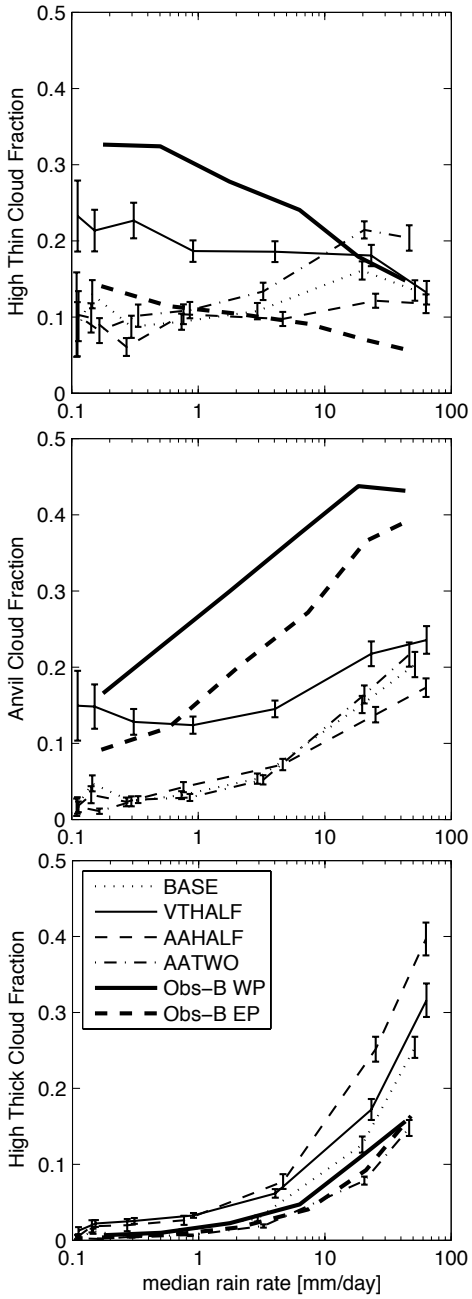

Fig. 5 As in Fig. 2, except that the thin lines are for the 2-D simulations BASE, VTHALF, AAHALF and AATWO. Heavy lines again represent observations for the EP and WP.

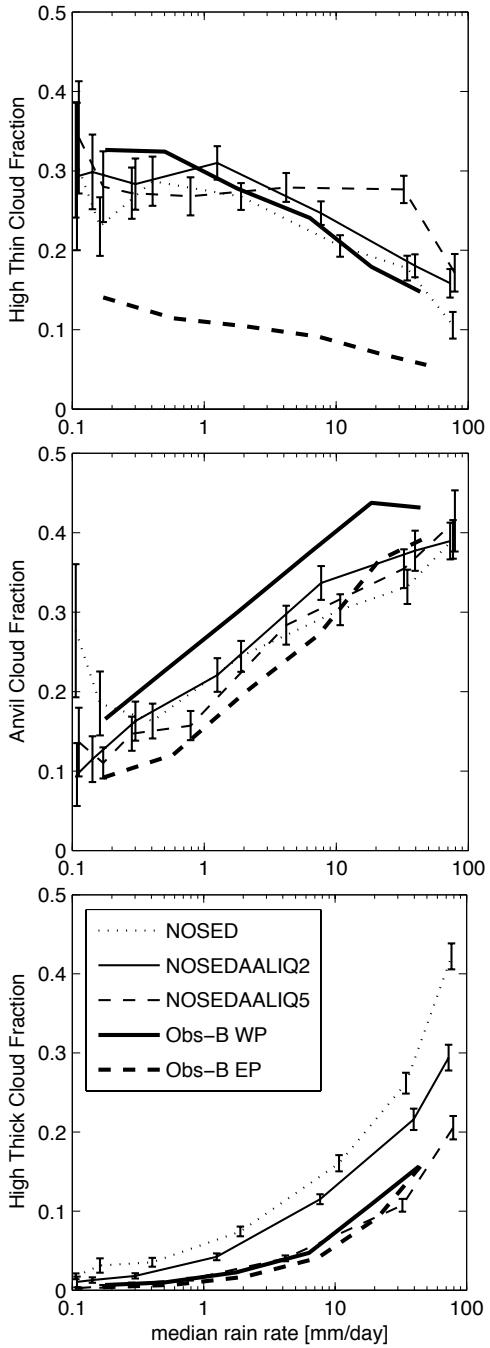

Fig. 6 As in Fig. 2, except that the thin lines are for the 2-D simulations NOSED, NOSEDAALIQ2, and NOSEDAALIQ5. Heavy lines again represent observations for the EP and WP.

Table 1. Domain Averages from observations and SAM for the WP and EP.

	Obs-B WP	SAM WP	Obs-B EP	SAM EP
Rain Rate (mm/day)	8.2	14.7	8.9	15. 0
High Thin Cloud Fraction	0.29	0.28	0.10	0.16
Anvil Cloud Fraction	0.31	0.11	0.23	0.09
High Thick Cloud Fraction	0.05	0.06	0.04	0.06
Anvil to High Thick Ratio	6.6	1.8	5.2	1.4
Albedo	0.38	0.25	0.39	0.26
OLR (Wm^{-2})	183.	223.	220.	243.

Table 2 : Descriptions of 2-D experiments. All changes are relative to BASE.

Run	**Description**
BASE	Default 2-D simulation: See text.
VTHALF	Reduce cloud ice fall speed by half.
AAHALF	Decrease rates of autoconversion and accretion for liquid and ice by half
AATWO	Increase rates of autoconversion and accretion for liquid and ice by factor of 2
AATEN	Increase rates of autoconversion and accretion for liquid and ice by factor of 10
HALFICE	Decrease rates of autoconversion and accretion for ice only by factor of 2
TWOICE	Increase rates of autoconversion and accretion for ice only by factor of 2
NOGRAU	Eliminate graupel as a hydrometeor species
HORRES 1	Increase horizontal resolution to 1 km
HORRES 0.5	Increase horizontal resolution to 0.5 km
VERTRES	Use 200 m horizontal resolution throughout the ice cloud layer
BIG	Double size of horizontal domain to 8192 km.
NOSED	No ice sedimentation, lower ice autoconversion threshold by factor of 100.
NOSEDAALIQ5	No ice sedimentation, lower ice autoconversion threshold by factor of 100. Increase autoconversion and accretion rates for liquid water by a factor of 5.

Table 3. Comparison of original WP and EP 3D experiments with WP2, in which the cloud physics specifications of experiment NOSEDAALIQ5 are used. Surface latent (LE) and sensible (SH) fluxes and the net flux into the ocean (Q_{ocean}) are listed.

Experiment	WP2	WP	EP
Precip. (mm day^{-1})	14.58	14.64	15.30
Cloud Fraction	0.89	0.60	0.59
Precipitable Water (mm)	84.96	79.68	87.42
Cloud Water Path (mm)	38.95	95.62	144.12
Ice Water Path (mm)	82.40	88.40	58.12
SST (˚K)	302.49	302.49	302.49
LE (W m^{-2})	62.21	71.06	44.84
SH (W m^{-2})	5.01	5.03	2.35
Q_{ocean} (W m^{-2})	87.34	102.34	128.89
SWCF (W m^{-2})	-98.49	-69.05	-74.65
LWCF (W m^{-2})	93.07	48.38	31.77
OLR (W m^{-2})	174.80	223.53	242.82
Albedo	0.32	0.25	0.26